Seasonal shifts in hydroclimate and 21st century warming in Western North America

Benjamin I Cook *

NASA Goddard Institute for Space Studies, NY, NY, USA

Lamont-Doherty Earth Observatory, Palisades, NY, USA

Richard Seager

Lamont-Doherty Earth Observatory, Palisades, NY, USA

Dorian J Burnette

University of Memphis, Memphis, TN, USA

Andrea J Ray

NOAA Earth System Research Lab, Boulder, CO, USA

* *Corresponding author address:* Benjamin I Cook, NASA Goddard Institute for Space Studies, 2880 Broadway, New York, NY 10025.

E-mail: benjamin.i.cook@nasa.gov, bc9z@ldeo.columbia.edu

ABSTRACT

Hydroclimate in Western North America (WNA) is highly seasonal, with ecological and social systems finely tuned to within year variations in moisture availability. Here, 21st century century climate model projections are used to assess seasonal changes in precipitation, evapotranspiration, and runoff in response to greenhouse gas warming across the diverse climates of WNA. Winter precipitation increases across most of WNA, but declines sharply in Mexico. During the spring, precipitation increases in the Northwest and Northern Plains and the drying in Mexico expands northward into the Southwest and California. Summer precipitation decreases over the Great Plains, the Pacific Northwest, and during July in the North American Monsoon region; this delay in the monsoon is largely compensated by increased late monsoon (September) precipitation. For most regions of WNA, these precipitation changes manifest as an amplification of precipitation seasonality (i.e., wetter wet seasons, drier dry seasons) and are forced by changes in moisture convergence due to changes in the mean flow or transient eddy activity. Even in areas where total winter precipitation (rain and snow) increases, snowfall is reduced, especially over the Montane West and Northwest Coastal regions. This shift from snow to rain, combined with increased spring-time evapotranspiration, increases runoff during the winter and decreases runoff in the spring. Notably, these large seasonal trends in precipitation and runoff over the 21st century are masked or obfuscated over much of WNA when integrated over the entire calendar year. Adaptation decisions will therefore need to account not only for declines in total water resources, but also shifts in hydroclimate within the calendar year.

1. Introduction

Climate change is a significant challenge for water resource management in Western North America (WNA) (e.g., Gleick 2010; MacDonald 2010; Scanlon et al. 2012). In this region, warming from increased greenhouse gas (GHG) forcing is expected to increase evaporative demand (Scheff and Frierson 2013), shift precipitation patterns (Seager and Vecchi 2010; Seager et al. 2013), and cause declines in runoff and streamflow (Hagemann et al. 2013; Schewe et al. 2013). Concerns about climate change in WNA have been amplified by several recent drought events, including Texas and northern Mexico in 2011 (Hoerling et al. 2012; Seager et al. 2014 in review), the Central Plains in 2012 (Hoerling et al. 2014), and the ongoing, chronic drought in the Southwest that began in 1998 (Cayan et al. 2010; Seager 2007; Weiss et al. 2009). But while climate model projections have been broadly analyzed to assess general declines in precipitation and water resources in WNA (e.g., Cayan et al. 2010; Seager et al. 2014 in review), little work has been done to comprehensively assess the seasonality of hydroclimate trends across the entire WNA domain.

Hydroclimate in WNA is highly seasonal (Markham 1970), perhaps best characterized by the pronounced wet and dry seasons evident in the seasonal distribution of precipitation (Figure 1, data from Schneider et al. 2014). In the coastal regions of the Northwest (127°W–118°W, 42°N–50°N) and Southwest (127°W–118°W, 33°N–42°N), most precipitation falls during the winter and spring (October–March). At lower elevations, where most precipitation falls as rain, annual peak runoff and reservoir inflow closely follow this annual precipitation maximum (Chang and Jung 2010; Dettinger et al. 2011). At higher elevations, where more precipitation occurs as snow, runoff and streamflow peaks shift later in the year, coinciding with the spring snow melt pulse (Aguado et al. 1992). Precipitation in the Montane West (118°W–106°W, 35°N–45°N), by contrast, has a more uniform seasonal distribution (Markham 1970; Mock 1996). In this area, most winter precipitation falls as snow, which accumulates and melts in the spring to drive the annual spring discharge peak and filling of reservoirs in rivers like the Colorado and upper basin of the Rio Grande (Christensen et al. 2004; Dahm et al. 2005). In the Northern (114°W–96°W, 45°N–53°N) and Central Plains (104°W–95°W, 30°N–45°N), peak annual precipitation occurs in the late spring and early summer. Modest snowfall during the winter, combined with this late spring/early summer precipitation peak, both contribute to spring-time maxima in runoff, especially for more northern rivers (e.g., the Red River in North Dakota, Stoner et al. 1993). Finally, the North American Monsoon region (112°W–102°W, 18°N–33°N) receives most of it's precipitation during the late summer and early fall. Here, over 70% of annual precipitation falls in July-August-September, causing large runoff peaks and river flows in September and October (Adams and Comrie 1997).

Even with no change in total annual water resources, shifts in hydroclimate and water availability at the seasonal scale can significantly impact the functioning of ecosystems and societies. Warm and cold season precipitation often satisfy different societal demands (e.g., reservoir supply vs dryland agriculture and ranching; Woodhouse et al. 2013), fire and ecosystem disturbance regimes are sensitive to the timing and amount of precipitation (Ray et al. 2007; Swetnam and Betancourt 1998), and shifts in runoff often require tradeoffs between managing reservoirs for flood control versus storage (Aguado et al. 1992; Dettinger et al. 2011). Given the clear ecological and social consequences of seasonal changes in WNA hydroclimate, it is therefore important to understand how and why these shifts will occur under global warming. To address this goal, we use climate projections from the Coupled Model Intercomparison Project version 5 (CMIP5, Taylor et al. 2012) to comprehensively analyze the seasonal response of hydroclimate in WNA over the 21st century. We expand on previous work (e.g., Cayan et al. 2010; Seager et al. 2013, 2014 in review) by focusing on the main terms in the surface moisture budget (precipitation, evapotranspiration, runoff) at the seasonal scale and across the diverse climates of WNA.

2. Methods and Data

a. CMIP5 Models

Our analyses use model output (1980–2099) from the historical and RCP 8.5 model scenarios in the CMIP5 archive (Taylor et al. 2012). The historical simulations use observationally derived climate forcings (e.g., solar, aerosols, greenhouse gases, etc) to force coupled ocean-atmosphere model simulations from 1850–2005. Simulations under the RCP 8.5 scenario are initialized using the end of the historical runs, and represent the high end of the suite of possible future GHG forcing scenarios. In RCP 8.5, the simulations are designed to have an approximate global radiative imbalance of +8.5 W m^{-2} at 2100. Use of RCP 8.5, rather than a lower emissions scenario, is appropriate, given the current lack of any serious international effort to mitigate GHG emissions.

We focus on variables that make up the surface moisture balance and are most relevant from an impacts and resource use perspective: precipitation (rain and snow), evapotranspiration, and runoff (surface and subsurface). Total precipitation (rain and snow) represents the moisture supply side of the surface moisture budget, which is then lost from the soil either vertically to the atmosphere (via evapotranspiration) or horizontally (via surface or subsurface runoff). Evapotranspiration rates depend on both the atmospheric demand for moisture (potential evapotranspiration), which is expected to increase with GHG warming, and soil moisture availability, which may increase or decrease depending on supply and demand changes. Runoff is an especially important variable from a resource use perspective, as it represents the total sustainable water supply (excluding renewable groundwater) available for use by local human populations (e.g., Murray et al. 2012; Postel et al. 1996; Vörösmarty et al. 2000). Runoff, and its seasonal cycle, is also critical for the ecological vitality of riparian ecosystems (Perry et al. 2012; Rood et al. 2008). We did not analyze soil moisture changes, because of the paucity of models that provided level-by-level soil moisture diagnostics for the RCP 8.5 simulations in the CMIP5 archive. Our analysis is therefore restricted to those models with continuous (historical to RCP 8.5) ensemble members (Table 1) that provide these hydroclimate diagnostics. With this criteria, we were able to analyze 22 total models, 8 of which have multiple ensemble members.

b. Analysis

The six regions of WNA that we focus on are: the Northwest Coast, the Southwest Coast, the Montane West, the Northern Plains, the Central Plains, and the North American Monsoon. These regions were chosen based on their distinct hydroclimate regimes and importance of water resources for local ecosystems, agriculture, and societies. These regions, including their hydroclimatology, are described in the Introduction and are indicated by the dashed boxes in Figure 1 and subsequent figures. For the spatial comparisons, all model diagnostics are interpolated to a common 2^{o} latitude/longitude grid. Within model ensemble averages are calculated before calculating the multi-model means so that each model is weighted equally. For the maps, areas where the multi-model ensemble shows *robust* changes, defined as at least 18 of 22 (80%) of individual models agreeing with the sign of the multi-model mean change, are indicated with a black x. For precipitation, snowfall, evapotranspiration, and runoff, areas where changes in the multi-model mean are small ($< 5\%$) are masked in gray, regardless of whether these changes are robust across models or not. For other plots, the multi-model mean is indicated by either a solid black line or colored bar, and the multi-model ensemble spread (+/-1 standard deviation) is shown by gray shading (line plots) or whiskers (bar plots). Seasonal averages are based on the water year (October-September), rather than the calendar year. We analyze changes in hydroclimate for two different 21st century intervals: 2030–2049 and 2080–2099, both relative to the historical model scenario baseline of 1980–1999. The historical baseline period is chosen so that projections reflect changes relative to the modern climate. For future projections, the later period (2080–2099) is chosen because the climate change signal is largest and clearest, while the former period (2030–2049) is more relevant to current and future efforts to develop plans for adaptation to climate change.

3. Projected changes in hydroclimate seasonality across North America

a. Spatial Patterns

Robust changes in annual average precipitation occur over Mexico (drier), the Eastern United States (wetter), and the northern half of North America (wetter) (Figure 2a,b). Changes in annual runoff are less robust (Figure 2c,d), increasing in the Northwest and Northeast and declining in a narrow band extending from Mexico up through New Mexico, Texas, and Colorado. Despite these large localized changes, annual average shifts in precipitation and runoff are small or non-robust across much of WNA.

Seasonal changes in hydroclimate are larger and more spatially extensive. Temperature (Figure 3) and precipitation (rain and snow, Figure 4) changes in our multi-model ensemble are generally consistent with other analyses of the CMIP5 model projections (e.g., Knutti and Sedlacek 2013). The temperature response is one of uniform and robust warming across the entire continent, with the largest magnitude of warming at high latitudes during the winter (JFM). The models also show hotspots of amplified warming in certain WNA regions, including the Montane West, Central Plains, and North American Monsoon. Precipitation reductions are most widespread and robust across models during winter and spring (AMJ). In winter, these declines are confined primarily to southern Arizona, New Mexico, Texas, Mexico, and Central America. By the spring this drying spreads northwest into Arizona, New Mexico, Colorado, Utah, Nevada, and California. During summer (JAS) and fall (OND), areas of reduced precipitation are less extensive, and in JAS, shifted northward to the Northwest Coast, and Central and Northern Plains. Widespread increases in precipitation are apparent across the fall, winter, and spring seasons over the northern half of the continent.

Despite increases in cold season total precipitation over broad areas (Figure 4), the amount falling as snow actually decreases across much of North America (Figure 5). The most widespread and robust declines occur in late fall/early winter (November-December) and late winter/early spring, seasons when warming can shorten the time when temperatures are ideal for snow (March-April). Largest declines in snowfall span from the West Coast and Montane West regions across the continent and into the Northeast. Increases in snowfall are confined to the most northerly latitudes around Hudson Bay, with little change in the Northern Plains during the core winter season (January-February).

Evapotranspiration increases over most of North America (Figure 6) in areas where moisture supply at the surface is sufficient to keep pace with the increased evaporative demand of a warmer atmosphere (Figure 3). Robust declines in evapotranspiration are confined primarily to the Southwest and Mexico; despite increases in evaporative demand, these are areas where soil moisture is expected to decline to the point that evapotranspiration rates become limited by soil moisture supply versus atmospheric demand (e.g., Seager et al. 2013). The largest runoff declines occur during the spring (Figure 7), spanning a broad area from the Northwest Coast, through California and the Montane West, and into the Southwest and Mexico. At high Northern latitudes, runoff increases during fall and winter, in step with large precipitation increases in these areas. Winter also sees modest increases in runoff over the Northwest and Southwest Coastal regions.

b. The Southwest and Northwest Coastal Regions

For the Southwest and Northwest coastal regions (Figure 8), the model precipitation climatologies (black lines, 1980–1999) closely match the observed climatology (blue lines) calculated from version 6 of the Global Precipitation Climatology Centre (GPCC, Schneider et al. 2014). Both the models and observations show the wet winter and dry summer seasonal pattern typical of the West Coast. Biases in the model precipitation are positive for nearly all months, especially during the winter along the Southwest Coast. Model snowfall in these regions is only a minor fraction of total winter precipitation, resulting in highest runoff during February and March. Evapotranspiration peaks in the spring and early summer, when evaporative demand is high and surface moisture is still available.

Over the 21st century, precipitation is projected to increase during January and February along the Southwest Coast and from November through February in the Northwest (Figure 9), declining in the spring (April–May) in the Southwest and during the summer (July–August) in the Northwest. Despite the wet season getting wetter in terms of total precipitation, both regions experience large declines in the amount of precipitation falling as snow. For the Southwest coast the reductions are sufficient to actually reduce the number of months that this region experiences snow (cf. the snow fall climatology in Figure 8). With the winter precipitation increases and the increased evaporative demand from the warmer atmosphere, evapotranspiration rates also increase in the first 3–6 months of the calendar year. As a result of the precipitation, snow, and evapotranspiration changes, the seasonal cycle of runoff shifts earlier in the year: increasing in January-February (increased precipitation and more falling as rain) and decreasing in April-May (increased evapotranspiration, modestly reduced precipitation, and less snow pack storage carrying over from the winter).

c. The Northern and Central Plains

The model ensemble has a slight positive precipitation bias over the Northern and Central Plains, but otherwise the precipitation seasonality is well resolved by the models (Figure 10). Total precipitation is relatively low in the winter months compared to the warm season, but most winter precipitation falls as snow, especially in the Northern Plains. Evapotranspiration rates in the Plains regions peak in the late spring and early summer (May-July). In the Northern Plains, model runoff peaks in March and April, when the winter snow pack melts and evapotranspiration rates are low, consistent with streamflow observations in this region. In the Central Plains, peak runoff is shifted later and coincides more closely with the spring precipitation maxima, although there is a broad cross-model spread in simulated runoff for this region.

In the Northern Plains, precipitation increases in April-May, followed by robust reductions during July and August; a similar pattern is also seen for the Central Plains (Figure 11). These seasonal shifts in precipitation point to an overall intensification of the seasonal cycle of precipitation in this region (i.e., wetter springs and drier summers). Despite increases in total winter and spring precipitation, snowfall declines in all months. Evapotranspiration shifts follow changes in precipitation, with increases in winter and spring and declines over the summer, pointing to the importance of both evaporative demand and moisture supply controls on evapotranspiration rates in these regions. Runoff changes are small or negligible for most months in the Northern Plains region; increases are apparent in January and

February, followed by declines in the spring (March-April). In the Central Plains, runoff decreases in nearly all months.

d. The Montane West and The North American Monsoon Region

For the Montane West and North American Monsoon regions, the models have substantial positive precipitation biases, especially during the winter in the North American Monsoon region and all year in the Montane West (Figure 12). Model wet biases in the Montane West may be caused by the relatively coarse horizontal resolutions of the GCMs, hampering the ability of the models to resolve the Sierra Nevada and Cascade mountain ranges and the necessary orographic effects on precipitation. Alternatively, the large mismatch in the Montane West may be due at least partially to problems in the observations, rather than the models. For example, precipitation datasets are known to have deficiencies in mountainous areas because of snow undercatch and station placement lower than most of the topography (e.g., Bosilovich et al. 2008; Legates and DeLiberty 1993), which may lead to large underestimates of precipitation. Comparisons we conducted against other precipitation datasets (e.g., PRISM) show similar, but less severe, dry biases in the observations (not shown). Over the North American Monsoon region the models also have difficulty capturing the rapid seasonal transitions into and out of the main monsoon season (July–September, Adams and Comrie 1997). Despite these differences, the models reasonably capture the seasonality, with precipitation evenly distribution throughout the year in the Montane West and concentrated during the summer in the North American Monsoon. In the Montane West, snow makes up most of the model winter precipitation, with subsequent melt in the spring leading to a pronounced runoff peak in March-April-May. Winter precipitation falls almost entirely as rain in the North American Monsoon region, causing a small runoff peak during the winter that is secondary to the dominant peak in August and September that follows the monsoon season rains.

Total winter precipitation increases in the Montane West (Figure 13), but this is matched by an almost equivalent decline in snowfall, indicating, as with other regions of WNA, an increased proportion of precipitation falling as rain rather than snow. The shift from snow to rain, combined with increased evapotranspiration during the spring, leads to a shift in runoff from spring (decreased) to winter (increased). The North American Monsoon region shows clear and consistent declines in precipitation in the winter and spring, forcing a large reduction in evapotranspiration during the spring. During the monsoon season, however, there is a decline in precipitation during the early part of the monsoon (July), and a general increase towards the end (September), indicating a delayed onset and withdrawal of the monsoon. Overall, the declines in winter and spring precipitation in this region lead to declines in runoff, especially during the winter and spring seasons.

e. Relationship to changes in atmospheric moisture budget and circulation

The diverse precipitation response in the models across regions and seasons can be attributed to various dynamic and thermodynamic mechanisms; a comprehensive analysis of these processes for North American precipitation trends in the CMIP5 projections is described in Seager et al. (2014 in review). To investigate these mechanisms in the context of our ensemble mean precipitation changes, we calculated climatologies and changes in mean flow and transient eddy moisture convergence for our three month seasonal composites. Only 17 (indicated by * in Table 1) of our original 22 models provided the necessary diagnostics. Areas of robust cross-model agreement for these variables are based on 13 of the 17 models. Seager et al. (2014 in review) compare the multimodel ensemble mean CMIP5 moisture budget with that in the European Centre for Medium Range Weather Forecasts Interim Reanalysis (ERA-I) and show a quite high level of model fidelity in simulating the main features.

As with other components of western hydroclimate, there is substantial seasonality in moisture convergence, illustrated by the climatology from the multi-model mean of our historical ensemble (Figure 14, 1980–1999). Transient eddies and the mean flow both converge moisture along the west coast during the cold season (OND and JFM). In the same seasons, the mean flow diverges moisture out of the Southwest and North American Monsoon region. During spring and summer, this region of mean flow divergence expands and shifts north, suppressing precipitation and drying California and the Montane West. Over the Central Plains and North American Monsoon regions, mean flow and transient eddy transports change sign during the observed seasonal cycle, with the mean flow converging moisture during the spring and summer wet seasons and diverging moisture during the fall and winter in these regions and with the transient eddies generally opposing the mean flow contribution.

Changes in the moisture convergence terms by the end of the 21st century generally reflect an intensification of these patterns (Figure 15). Reductions in cold season (OND and JFM) precipitation over Mexico and the Southwest are caused primarily by enhanced mean flow divergence. Following the climatology, in the spring (AMJ) the center of enhanced mean flow divergence shifts and spreads north, allowing the drying to expand across the Montane West and West Coast. Changes in the mean flow also drive the intensification of precipitation seasonality in the Northwest, with enhanced mean flow moisture convergence in OND and JFM in this region (the wet season), followed by anomalous divergence that persists through the spring and summer (the dry season). While mean flow shifts dominate precipitation changes over the far western half of the continent, changes in transient eddy moisture fluxes are the main actor in the Plains regions. In JFM, precipitation increases in the Northern Plains because of increased moisture convergence by transient eddies, while during JAS the mean pattern of transient eddy moisture convergence (centered in eastern Mexico) and divergence (from Plains and east) intensifies and shifts northward, drying out the Central and Northern Plains. As shown in Seager et al. (2014 in review), the intensifications of transient eddy moisture convergences and divergences arises not from stronger eddy fields (at lower levels they actually weaken) but from the intensified moisture gradients expected with a warming atmosphere than can hold more moisture. Changes in transient eddy activity during OND break the broad tendency in the models to intensify the climatology with GHG warming. During this season, anomalous convergence in eastern Mexico and anomalous divergence across the North American Monsoon and Central Plains regions actually oppose the OND climatology. This may indicate a tendency in the model for GHG warming to extend the JAS climatological pattern of transient eddy moisture convergence/divergence later in the year. Alternatively, this pattern could reflect a poleward shift in the transient eddy field during the fall across North America (Simpson et al. 2014).

In addition to the mean flow induced drying over the North American Monsoon region during the cold season, precipitation during the summer shows an overall shift towards delayed monsoon onset and withdrawal. This shift in monsoon seasonality has been documented previously in CMIP5 model simulations for global monsoon regions, including North

American (Cook and Seager 2013; Lee and Wang 2014; Seth et al. 2011, 2013). Drying and warming in the winter and spring creates an enhanced convective barrier, suppressing precipitation and delaying the monsoon onset. Once the monsoon becomes fully established, however, the surface is warm and moist enough to overcome the increased stability constraint, and precipitation increases.

4. Impacts on water resources, ecosystems, and landscapes of future changes in seasonality

The changes in seasonality identified here will have important consequences for fauna and flora, ecological and riparian systems, water resources, and resource management efforts in WNA. Climate change in WNA will likely diminish total water resources, with important ramifications for agriculture, municipalities, and natural resource management (Hagemann et al. 2013; Schewe et al. 2013; Seager and Vecchi 2010; Seager et al. 2013). But management and adaptation initiatives to address these changes will also need to account for large sub-annual redistributions and shifts in seasonality of the same water resources. Indeed, there is evidence that these seasonal hydroclimate changes may already be occurring (e.g., Fritze et al. 2011; Pederson et al. 2011; Polley et al. 2013; Stewart et al. 2005). As they unfold they will have significant impacts on the ecological and social systems in the region. Of particular concern is the widespread decrease in spring runoff and the more general drop in runoff in the Central Plains and monsoon region. These runoff changes will impact river flows in the spring and summer with consequences for riparian ecosystems and the wildlife that depend on them, including migratory birds (Perry et al. 2012).

Other impacts are also likely. Reductions in snowfall and a shift from snow to rain will likely have negative impacts on winter tourism (e.g., skiing, snowboarding; Scott and McBoyle 2007; Elsasser et al. 2002), and may even depress residential property prices and employment in areas reliant on this seasonal income (Butsic et al. 2011). Combined with increased evapotranspiration rates in the spring, these snowfall changes are also expected to shift runoff from spring to winter. Critically, this runoff is important for refilling reservoirs that provide water for agricultural and municipal needs throughout the year. During winter, however, reservoirs are often operated in flood protection mode, which means that this earlier runoff may not be captured and stored for later use (Barnett et al. 2005; Fritze et al. 2011). If reservoir management does not adapt and account for this change in runoff seasonality, effective water availability will decline even if total annual runoff is the same.

North of Mexico, increases in evapotranspiration and declines in warm season precipitation (spring and summer) are likely to have significant effects on important breeding and migration habitats for a variety of species. The Northern Plains, for example, hosts the Prairie Potholes wetlands, the primary breeding site for most of North America's duck populations. The projected climate changes documented in this study, however, will act to dry out these wetlands in summer and degrade this habitat, with expected negative impacts on duck populations (Ballard et al. in press; Johnson et al. 2005). Such climatic shifts are likely to affect other important hydroclimate-sensitive wildlife habitats as well, including the Salton Sea in California (Cohn 2000; Kaiser 1999), the 'Sky Islands' of the Southwest (Coe et al. 2012), and riparian habitats throughout WNA (Perry et al. 2012).

Fire activity in WNA is also expected to increase with climate change, and can be linked to some of the projected seasonality changes. For example, wildfire activity and the length of the fire season increases with earlier snow melt, as well as warmer temperatures and drought (e.g., Marlon et al. 2012; Stephens et al. 2013; Westerling et al. 2006). In the North American Monsoon region the fire season usually ends with the first monsoon rains (Ray et al. 2007; Swetnam and Betancourt 1998); the projected delayed onset of the monsoon will thus contribute to extending the fire season in this region.

Finally, seasonal hydroclimate shifts are also likely to have significant impacts on rangelands and livestock production. Seasonal changes in moisture availability alter the competitive landscape in grasslands, affecting plant community composition and competitive interactions (Polley et al. 2013; Robertson et al. 2010). Within year variations in rangeland productivity, and thus food availability for grazing species, is often tightly coupled with seasonal variations in precipitation and evaporative demand (Polley et al. 2010). And changes in precipitation seasonality may even have direct effects on livestock weight gain through effects on forage quality (Craine et al. 2009, 2012). Given the shifts documented here, it is expected that rangeland quality and livestock production will increase with warmer and wetter conditions in the Northern Plains, while declining across the Southwest, Southern and Central Plains, and even in the Northwest where summer season drought will inhibit productivity (Polley et al. 2013).

5. Conclusions

The CMIP5 models reproduce the observed seasonality of precipitation and runoff across the diverse climates of WNA, providing an opportunity to investigate seasonal scale hydroclimate responses to greenhouse warming over the coming century. In aggregate, these models point to an overall intensification of hydroclimate seasonality (wet seasons getting wetter and dry seasons getting drier), and a shift in timing of runoff and precipitation. These large seasonal trends are masked when analyzing annual average quantities, and can be attributed to physical processes that vary across seasons and regions of WNA.

The largest and most consistent responses in the multi-model ensemble are a 1) continental scale warming in all seasons, 2) increased evapotranspiration from fall to spring north of Mexico, 3) decreased winter and spring evapotranspiration in Mexico, and a 4) shift from snow to rain during the cold season months. To first order, these changes are a direct response to the greenhouse gas forced warming of the atmosphere. Projections of these variables may thus be considered more robust relative to other variables for which there are larger uncertainties and greater spread across ensemble members. Runoff decreases in the spring and increases in the winter, a result of both increased evapotranspiration in the spring and the shift in cold season precipitation from snow to rain.

Effectively addressing these challenges will require a number of strategies. Reservoir management, for example, may be adjusted to better capture earlier runoff, at least up to a point. Increases in fire frequency and severity, and resulting costs to forests and grasslands and life and property, may be mitigated through proactive land management and planning. Efforts to conserve landscapes, ecosystems and species will need to take careful account of how shifts in seasonality will alter the environments and the likelihood for success of conservation efforts. Such decision-making will address much smaller spatial scales than we do here. On the other hand the changes in seasonality identified here are large scale, coherent and robust across models and, hence, these results could be used as a first-order guide for adaptation strategies across many sectors.

Acknowledgments.

BI Cook acknowledges the support of National Aeronautics and Space Administration Modeling Analysis and Prediction Program. Naomi Henderson and Haibo Liu provided invaluable computing support at LDEO. RS was supported by NSF award AGS-1243204 ("Linking near-term future changes in weather and hydroclimate in western North America to adaptation for ecosystem and land management") and DOE award DE-SC0005107. Lamont contribution #.

REFERENCES

Adams, D. K. and A. C. Comrie, 1997: The North American Monsoon. *Bulletin of the American Meteorological Society*, **78 (10)**, 2197–2213.

Aguado, E., D. Cayan, L. Riddle, and M. Roos, 1992: Climatic Fluctuations and the Timing of West Coast Streamflow. *Journal of Climate*, **5 (12)**, 1468–1483, doi:10.1175/1520-0442(1992)005⟨1468:CFATTO⟩2.0.CO;2.

Ballard, T., et al., in press: Hydroclimate Variability and Change in the Prairie Pothole Region, the "Duck Factory" of North America. *Earth Interactions*.

Barnett, T. P., J. C. Adam, and D. P. Lettenmaier, 2005: Potential impacts of a warming climate on water availability in snow-dominated regions. *Nature*, **438 (7066)**, 303–309.

Bosilovich, M. G., J. Chen, F. R. Robertson, and R. F. Adler, 2008: Evaluation of Global Precipitation in Reanalyses. *Journal of Applied Meteorology and Climatology*, **47 (9)**, 2279–2299, doi:10.1175/2008JAMC1921.1.

Butsic, V., E. Hanak, and R. G. Valletta, 2011: Climate Change and Housing Prices: Hedonic Estimates for Ski Resorts in Western North America. *Land Economics*, **87 (1)**, 75–91.

Cayan, D. R., T. Das, D. W. Pierce, T. P. Barnett, M. Tyree, and A. Gershunov, 2010: Future dryness in the southwest US and the hydrology of the early 21st century drought. *Proceedings of the National Academy of Sciences*, **107 (50)**, 21 271–21 276, doi:10.1073/pnas.0912391107.

Chang, H. and I.-W. Jung, 2010: Spatial and temporal changes in runoff caused by climate change in a complex large river basin in Oregon. *Journal of Hydrology*, **388 (3–4)**, 186 – 207, doi:http://dx.doi.org/10.1016/j.jhydrol.2010.04.040.

Christensen, N. S., A. W. Wood, N. Voisin, D. P. Lettenmaier, and R. N. Palmer, 2004: The Effects of Climate Change on the Hydrology and Water Resources of the Colorado River Basin. *Climatic Change*, **62 (1-3)**, 337–363, doi:10.1023/B:CLIM.0000013684.13621.1f.

Coe, S. J., D. M. Finch, and M. M. Friggens, 2012: An assessment of climate change and the vulnerability of wildlife in the Sky Islands of the Southwest. General Technical Report RMRS-GTR-273. Tech. rep., U.S. Department of Agriculture, Forest Service, Rocky Mountain Research Station, 208 pp.

Cohn, J. P., 2000: Saving the Salton Sea: Researchers work to understand its problems and provide possible solutions. *Bioscience*, **50 (4)**, 295–301.

Cook, B. I. and R. Seager, 2013: The response of the North American Monsoon to increased greenhouse gas forcing. *Journal of Geophysical Research: Atmospheres*, **118 (4)**, 1690–1699, doi:10.1002/jgrd.50111.

Craine, J. M., J. B. Nippert, A. J. Elmore, A. M. Skibbe, S. L. Hutchinson, and N. A. Brunsell, 2012: Timing of climate variability and grassland productivity. *Proceedings of the National Academy of Sciences*, **109 (9)**, 3401–3405, doi:10.1073/pnas.1118438109, URL `http://www.pnas.org/content/109/9/3401.abstract`, `http://www.pnas.org/content/109/9/3401.full.pdf+html`.

Craine, J. M., E. G. Towne, A. Joern, and R. G. Hamilton, 2009: Consequences of climate variability for the performance of bison in tallgrass prairie. *Global change biology*, **15 (3)**, 772–779, doi:10.1111/j.1365-2486.2008.01769.x.

Dahm, C. N., R. J. Edwards, and F. P. Gelwick, 2005: *Gulf Coast rivers of the southwestern United States.*, 181–228. Elsevier, Amsterdam.

Dettinger, M. D., F. M. Ralph, T. Das, P. J. Neiman, and D. R. Cayan, 2011: Atmospheric rivers, floods and the water resources of california. *Water*, **3 (2)**, 445–478, doi:10.3390/w3020445.

Elsasser, H., R. Bürki, et al., 2002: Climate change as a threat to tourism in the Alps. *Climate Research*, **20 (3)**, 253–257, doi:doi:10.3354/cr020253.

Fritze, H., I. T. Stewart, and E. Pebesma, 2011: Shifts in Western North American Snowmelt Runoff Regimes for the Recent Warm Decades. *Journal of Hydrometeorology*, **12 (5)**, 989–1006, doi:10.1175/2011JHM1360.1.

Gleick, P. H., 2010: Roadmap for sustainable water resources in southwestern North America. *Proceedings of the National Academy of Sciences*, **107 (50)**, 21 300–21 305, doi:10.1073/pnas.1005473107.

Hagemann, S., et al., 2013: Climate change impact on available water resources obtained using multiple global climate and hydrology models. *Earth System Dynamics*, **4 (1)**, 129–144, doi:10.5194/esd-4-129-2013.

Hoerling, M., J. Eischeid, A. Kumar, R. Leung, A. Mariotti, K. Mo, S. Schubert, and R. Seager, 2014: Causes and Predictability of the 2012 Great Plains Drought. *Bulletin* *of the American Meteorological Society*, **95**, 269–282, doi:doi:http://dx.doi.org/10.1175/BAMS-D-13-00055.1.

Hoerling, M., et al., 2012: Anatomy of an Extreme Event. *Journal of Climate*, **26 (9)**, 2811–2832, doi:10.1175/JCLI-D-12-00270.1.

Johnson, W. C., B. V. Millett, T. Gilmanov, R. A. Voldseth, G. R. Guntenspergen, and D. E. Naugle, 2005: Vulnerability of Northern Prairie Wetlands to Climate Change. *BioScience*, **55 (10)**, 863–872, doi:10.1641/0006-3568(2005)055[0863:VONPWT]2.0.CO;2.

Kaiser, J., 1999: Battle Over a Dying Sea. *Science*, **284 (5411)**, 28–30, doi:10.1126/science.284.5411.28, URL `http://www.sciencemag.org/content/284/5411/28.short`.

Knutti, R. and J. Sedlacek, 2013: Robustness and uncertainties in the new CMIP5 climate model projections. *Nature Climate Change*, **3 (4)**, 369–373, doi:10.1038/nclimate1716.

Lee, J.-Y. and B. Wang, 2014: Future change of global monsoon in the CMIP5. *Climate Dynamics*, **42 (1-2)**, 101–119, doi:10.1007/s00382-012-1564-0.

Legates, D. R. and T. L. DeLiberty, 1993: Precipitation Measurement Biases in the United States. *Journal of the American Water Resources Association*, **29 (5)**, 855–861, doi:10.1111/j.1752-1688.1993.tb03245.x.

MacDonald, G. M., 2010: Water, climate change, and sustainability in the southwest. *Proceedings of the National Academy of Sciences*, **107 (50)**, 21 256–21 262, doi:10.1073/pnas.0909651107.

Markham, C. G., 1970: Seasonality of Precipitation in the United States. *Annals of the Association of American Geographers*, **60 (3)**, 593–597, doi:10.1111/j.1467-8306.1970.tb00743.x.

Marlon, J. R., et al., 2012: Long-term perspective on wildfires in the western usa. *Proceedings of the National Academy of Sciences*, **109 (9)**, E535–E543, doi:10.1073/pnas.1112839109, URL `http://www.pnas.org/content/109/9/E535.abstract`, `http://www.pnas.org/content/109/9/E535.full.pdf+html`.

Mock, C. J., 1996: Climatic Controls and Spatial Variations of Precipitation in the Western United States. *Journal of Climate*, **9 (5)**, 1111–1125, doi:10.1175/1520-0442(1996)009⟨1111:CCASVO⟩2.0.CO;2.

Murray, S., P. Foster, and I. Prentice, 2012: Future global water resources with respect to climate change and water withdrawals as estimated by a dynamic global vegetation model. *Journal of Hydrology*, **448–449 (0)**, 14 – 29, doi:10.1016/j.jhydrol.2012.02.044, URL `http://www.sciencedirect.com/science/article/pii/S0022169412001692`.

Pederson, G. T., et al., 2011: The unusual nature of recent snowpack declines in the north american cordillera. *Science*, **333 (6040)**, 332–335, doi:10.1126/science.1201570.

Perry, L. G., D. C. Andersen, L. V. Reynolds, S. M. Nelson, and P. B. Shafroth, 2012: Vulnerability of riparian ecosystems to elevated CO2 and climate change in arid and semiarid western North America. *Global Change Biology*, **18 (3)**, 821–842, doi:10.1111/j.1365-2486.2011.02588.x.

Polley, H. W., D. D. Briske, J. A. Morgan, K. Wolter, D. W. Bailey, and J. R. Brown, 2013:

Climate Change and North American Rangelands: Trends, Projections, and Implications. *Rangeland Ecology & Management*, **66 (5)**, 493–511, doi:10.2111/REM-D-12-00068.1.

Polley, H. W., et al., 2010: Physiological and environmental regulation of interannual variability in CO2 exchange on rangelands in the western United States. *Global Change Biology*, **16 (3)**, 990–1002, doi:10.1111/j.1365-2486.2009.01966.x.

Postel, S. L., G. C. Daily, P. R. Ehrlich, et al., 1996: Human Appropriation of Renewable Fresh Water. *Science*, **271 (5250)**, 785–787.

Ray, A. J., G. M. Garfin, M. Wilder, M. Vásquez-León, M. Lenart, and A. C. Comrie, 2007: Applications of Monsoon Research: Opportunities to Inform Decision Making and Reduce Regional Vulnerability. *Journal of Climate*, **20 (9)**, 1608–1627, doi:10.1175/JCLI4098.1.

Robertson, T. R., J. C. Zak, and D. T. Tissue, 2010: Precipitation magnitude and timing differentially affect species richness and plant density in the sotol grassland of the Chihuahuan Desert. *Oecologia*, **162 (1)**, 185–197, doi:10.1007/s00442-009-1449-z.

Rood, S. B., J. Pan, K. M. Gill, C. G. Franks, G. M. Samuelson, and A. Shepherd, 2008: Declining summer flows of Rocky Mountain rivers: Changing seasonal hydrology and probable impacts on floodplain forests. *Journal of Hydrology*, **349 (3–4)**, 397 – 410, doi: http://dx.doi.org/10.1016/j.jhydrol.2007.11.012.

Scanlon, B. R., C. C. Faunt, L. Longuevergne, R. C. Reedy, W. M. Alley, V. L. McGuire, and P. B. McMahon, 2012: Groundwater depletion and sustainability of irrigation in the US High Plains and Central Valley. *Proceedings of the National Academy of Sciences*, **109 (24)**, 9320–9325, doi:10.1073/pnas.1200311109.

Scheff, J. and D. M. W. Frierson, 2013: Scaling Potential Evapotranspiration with Greenhouse Warming. *Journal of Climate*, doi:10.1175/JCLI-D-13-00233.1.

Schewe, J., et al., 2013: Multimodel assessment of water scarcity under climate change. *Proceedings of the National Academy of Sciences*, **Early Edition**, doi:10.1073/pnas.1222460110.

Schneider, U., A. Becker, P. Finger, A. Meyer-Christoffer, M. Ziese, and B. Rudolf, 2014: GPCC's new land surface precipitation climatology based on quality-controlled in situ data and its role in quantifying the global water cycle. *Theoretical and Applied Climatology*, **115 (1-2)**, 15–40, doi:10.1007/s00704-013-0860-x.

Scott, D. and G. McBoyle, 2007: Climate change adaptation in the ski industry. *Mitigation and Adaptation Strategies for Global Change*, **12 (8)**, 1411–1431, doi:10.1007/s11027-006-9071-4.

Seager, R., 2007: The Turn of the Century North American Drought: Global Context, Dynamics, and Past Analogs*. *Journal of Climate*, **20 (22)**, 5527–5552, doi:10.1175/2007JCLI1529.1.

Seager, R., M. Ting, C. Li, N. Naik, B. Cook, J. Nakamura, and H. Liu, 2013: Projections of declining surface-water availability for the southwestern United States. *Nature Climate Change*, **3**, 482–486, doi:10.1038/nclimate1787.

Seager, R. and G. A. Vecchi, 2010: Greenhouse warming and the 21st century hydroclimate of southwestern North America. *Proceedings of the National Academy of Sciences*, **107 (50)**, 21 277–21 282, doi:10.1073/pnas.0910856107.

Seager, R., et al., 2014 in review: Dynamical and thermodynamical causes of large-scale changes in the hydrological cycle over North America in response to global warming. *Journal of Climate*.

Seth, A., S. A. Rauscher, M. Biasutti, A. Giannini, S. J. Camargo, and M. Rojas, 2013: CMIP5 Projected Changes in the Annual Cycle of Precipitation in Monsoon Regions. *Journal of Climate*, **26 (19)**, 7328–7351, doi:10.1175/JCLI-D-12-00726.1.

Seth, A., S. A. Rauscher, M. Rojas, A. Giannini, and S. J. Camargo, 2011: Enhanced spring convective barrier for monsoons in a warmer world? *Climatic Change*, **104 (2)**, 403–414, doi:10.1007/s10584-010-9973-8.

Simpson, I. R., T. A. Shaw, and R. Seager, 2014: A diagnosis of the seasonally and longitudinally varying mid-latitude circulation response to global warming. *Journal of the Atmospheric Sciences*, **Early Online Release**, doi:doi:10.1175/JAS-D-13-0325.1.

Stephens, S. L., J. K. Agee, P. Z. Fulé, M. P. North, W. H. Romme, T. W. Swetnam, and M. G. Turner, 2013: Managing Forests and Fire in Changing Climates. *Science*, **342 (6154)**, 41–42, doi:10.1126/science.1240294, `http://www.sciencemag.org/content/342/6154/41.full.pdf`.

Stewart, I., D. Cayan, and M. Dettinger, 2005: Changes toward Earlier Streamflow Timing across Western North America. *Journal of Climate*, **18 (8)**, 1136–1155, doi:10.1175/JCLI3321.1.

Stoner, J. D., D. L. Lorenz, G. J. Wiche, and R. M. Goldstein, 1993: Red Rver of the North

Basin, Minnesota, North Dakota, and South Dakota. *JAWRA Journal of the American Water Resources Association*, **29 (4)**, 575–615, doi:10.1111/j.1752-1688.1993.tb03229.x.

Swetnam, T. W. and J. L. Betancourt, 1998: Mesoscale Disturbance and Ecological Response to Decadal Climatic Variability in the American Southwest. *Journal of Climate*, **11 (12)**, 3128–3147, doi:10.1175/1520-0442(1998)011⟨3128:MDAERT⟩2.0.CO;2.

Taylor, K. E., R. J. Stouffer, and G. A. Meehl, 2012: An Overview Of CMIP5 And The Experiment Design. *Bulletin of the American Meteorological Society*, **93 (4)**, 485–498, doi:http://dx.doi.org/10.1175/BAMS-D-11-00094.1.

Vörösmarty, C. J., P. Green, J. Salisbury, and R. B. Lammers, 2000: Global Water Resources: Vulnerability from Climate Change and Population Growth. *Science*, **289 (5477)**, 284–288, doi:10.1126/science.289.5477.284, URL `http://www.sciencemag.org/content/289/5477/284.abstract`.

Weiss, J. L., C. L. Castro, and J. T. Overpeck, 2009: Distinguishing Pronounced Droughts in the Southwestern United States: Seasonality and Effects of Warmer Temperatures. *Journal of Climate*, **22 (22)**, 5918–5932, doi:10.1175/2009JCLI2905.1.

Westerling, A. L., H. G. Hidalgo, D. R. Cayan, and T. W. Swetnam, 2006: Warming and Earlier Spring Increase Western U.S. Forest Wildfire Activity. *Science*, **313 (5789)**, 940–943, doi:10.1126/science.1128834, `http://www.sciencemag.org/content/313/5789/940.full.pdf`.

Woodhouse, C. A., D. M. Meko, D. Griffin, and C. L. Castro, 2013: Tree rings and multiseason drought variability in the lower Rio Grande Basin, USA. *Water Resources Re-*

search, **49 (2)**, 844–850, doi:10.1002/wrcr.20098, URL http://dx.doi.org/10.1002/wrcr.20098.

List of Tables

TABLE 1. Continuous model ensembles from the CMIP5 experiments (historical+RCP8.5) used in this analysis, including the modeling center or group that supplied the output, the number of ensemble members that met our criteria for inclusion, and the approximate spatial resolution. The 17 models labelled with * had the diagnostics available to calculate the moisture convergence terms related to the mean flow and transient eddies.

Model	Modeling Center (or Group)	# Runs	Lat/Lon Resolution
BCC-CSM1.1*	BCC[a]	1	2.8°x2.8°
BNU-ESM*	GCESS[b]	1	2.8°x2.8°
CanESM2*	CCCMA[c]	5	2.8°x2.8°
CCSM4*	NCAR[d]	6	0.94°x1.25°
CESM-BGC	NCAR[d]	1	0.94°x1.25°
CESM1-CAM5	NCAR[d]	3	0.94°x1.25°
CMCC-CM*	CMCC[e]	1	0.75°x0.75°
CNRM-CM5*	CNRM-CERFACS[f]	4	1.4°x1.4°
CSIRO-MK3.6.0*	CSIRO-QCCCE[g]	10	1.87°x1.87°
GFDL-ESM2G*	NOAA GFDL[h]	1	2.0°x2.5°
GFDL-ESM2M*	NOAA GFDL[h]	1	2.0°x2.5°
GISS-E2-H	NASA GISS[i]	2	2.0°x2.5°
GISS-E2-R	NASA GISS[i]	1	2.0°x2.5°
INMCM4.0*	INM[j]	1	1.5°x2.0°
IPSL-CM5B-LR*	IPSL[k]	1	1.9°x3.75°
MIROC5*	MIROC[l]	3	1.4°x1.4°
MIROC-ESM*	MIROC[m]	1	2.8°x2.8°
MIROC-ESM-CHEM*	MIROC[m]	1	2.8°x2.8°
MPI-ESM-LR*	MPI-M[n]	3	1.87°x1.87°
MRI-CGCM3*	MRI[o]	1	1.1°x1.1°
NorESM1-M*	NCC[p]	1	1.9°x2.5°
NorESM1-ME	NCC[p]	1	1.9°x2.5°

[a]Beijing Climate Center, China Meteorological Administration, [b]College of Global Change and Earth System Science, Beijing Normal University, [c]Canadian Centre for Climate Modelling and Analysis, [d]National Center for Atmospheric Research, [e]Centro Euro-Mediterraneo per I Cambiamenti Climatici, [f]Centre National de Recherches Météorologiques / Centre Européen de Recherche et Formation Avancée en Calcul Scientifique, [g]Commonwealth Scientific and Industrial Research Organization in collaboration with Queensland Climate Change Centre of Excellence, [h]NOAA Geophysical Fluid Dynamics Laboratory, [i]NASA Goddard Institute for Space Studies, [j]Institute for Numerical Mathematics, [k]Institut Pierre-Simon Laplace, [l]Atmosphere and Ocean Research Institute (The University of Tokyo), National Institute for Environmental Studies, and Japan Agency for Marine-Earth Science and Technology, [m]Japan Agency for Marine-Earth Science and Technology, Atmosphere and Ocean Research Institute (The University of Tokyo), and National Institute for Environmental Studies, [n]Max Planck Institute for Meteorology, [o]Meteorological Research Institute, [p]Norwegian Climate Centre

List of Figures

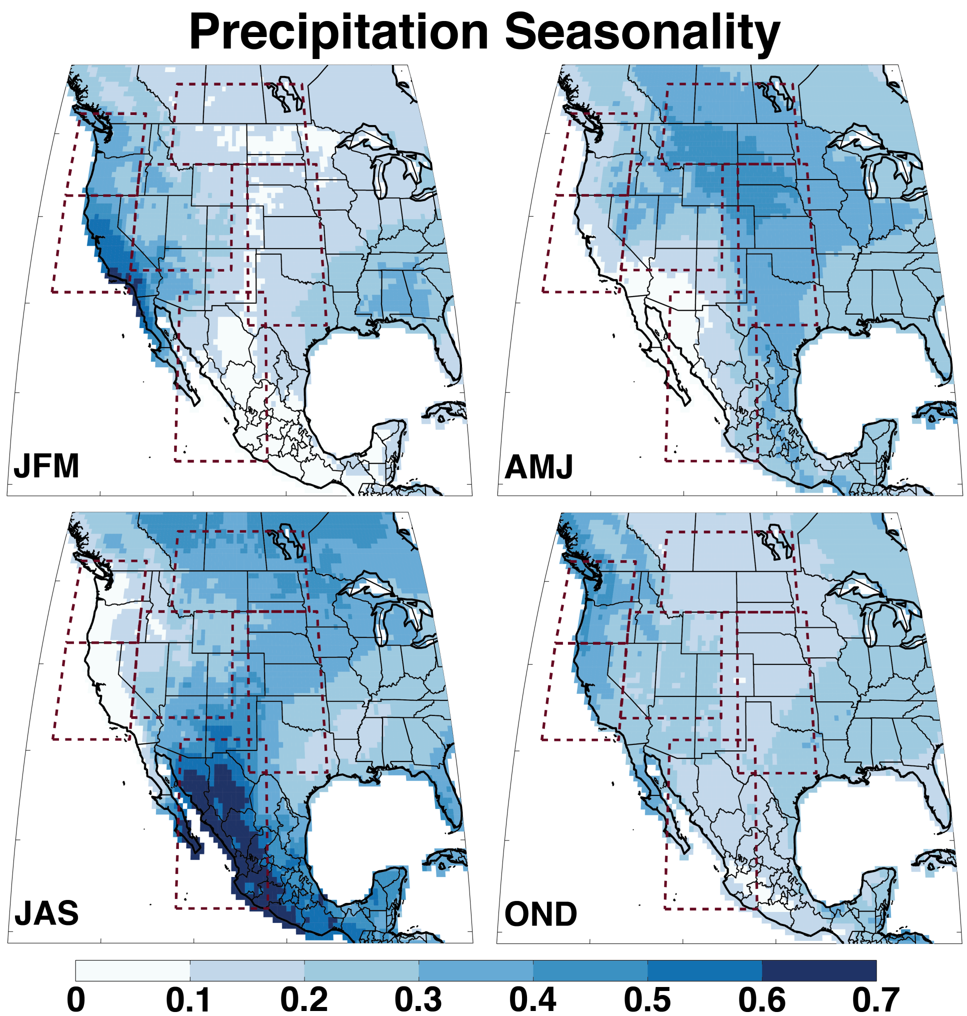

Fig. 1. Fraction of mean annual precipitation (1980–1999) falling within 3-month seasons. Data from GPCC version 6 precipitation dataset (Schneider et al. 2014). Regions that serve as the focus of this study are outlined in the dashed black lines: the Northwest Coast (127°W–118°W, 42°N–50°N), the Southwest Coast (127°W–118°W, 33°N–42°N), the Montane West (118°W–106°W, 35°N–45°N), the Northern Plains (114°W–96°W, 45°N–53°N), the Central Plains (104°W–95°W, 30°N–45°N), and the North American Monsoon (112°W–102°W, 18°N–33°N).

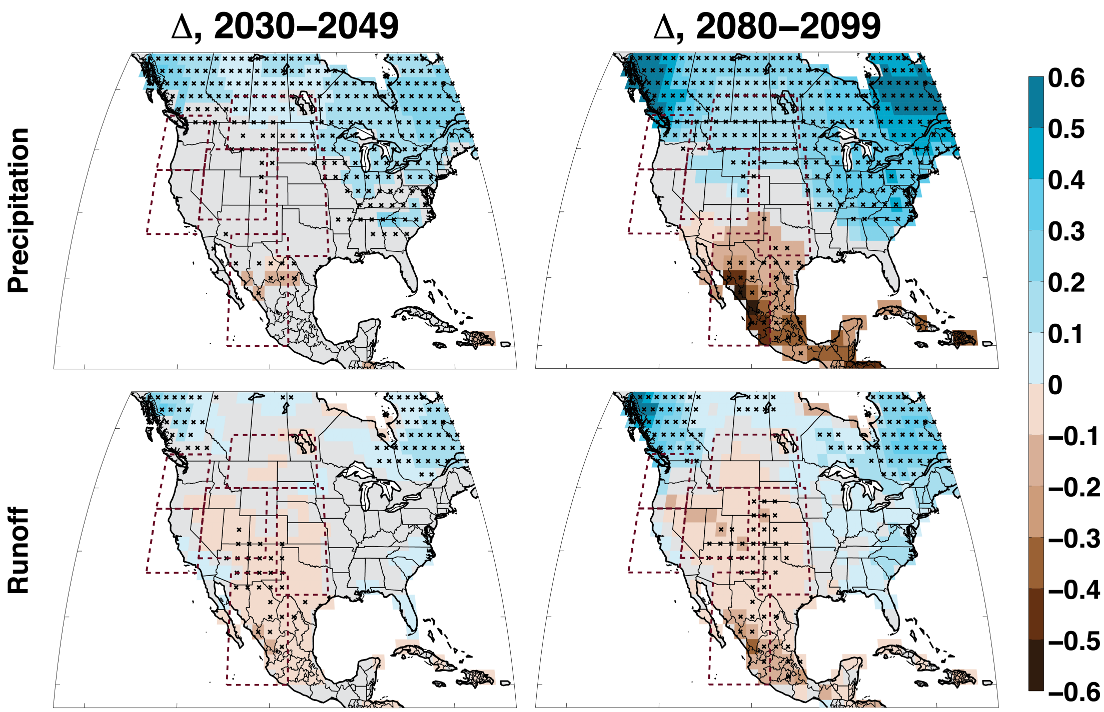

Fig. 2. Annual average changes in precipitation and total runoff (mm day^{-1}) in the RCP8.5 projections: 2030–2049 vs 1980-1999 (left column) and 2080–2099 vs 1980-1999 (right column). Areas marked with **x** indicate regions where changes in at least 18 of the 22 models (80%) agree with the sign of the change in the multi-model mean. Small changes (< 5%) in the multi-model mean are masked in gray.

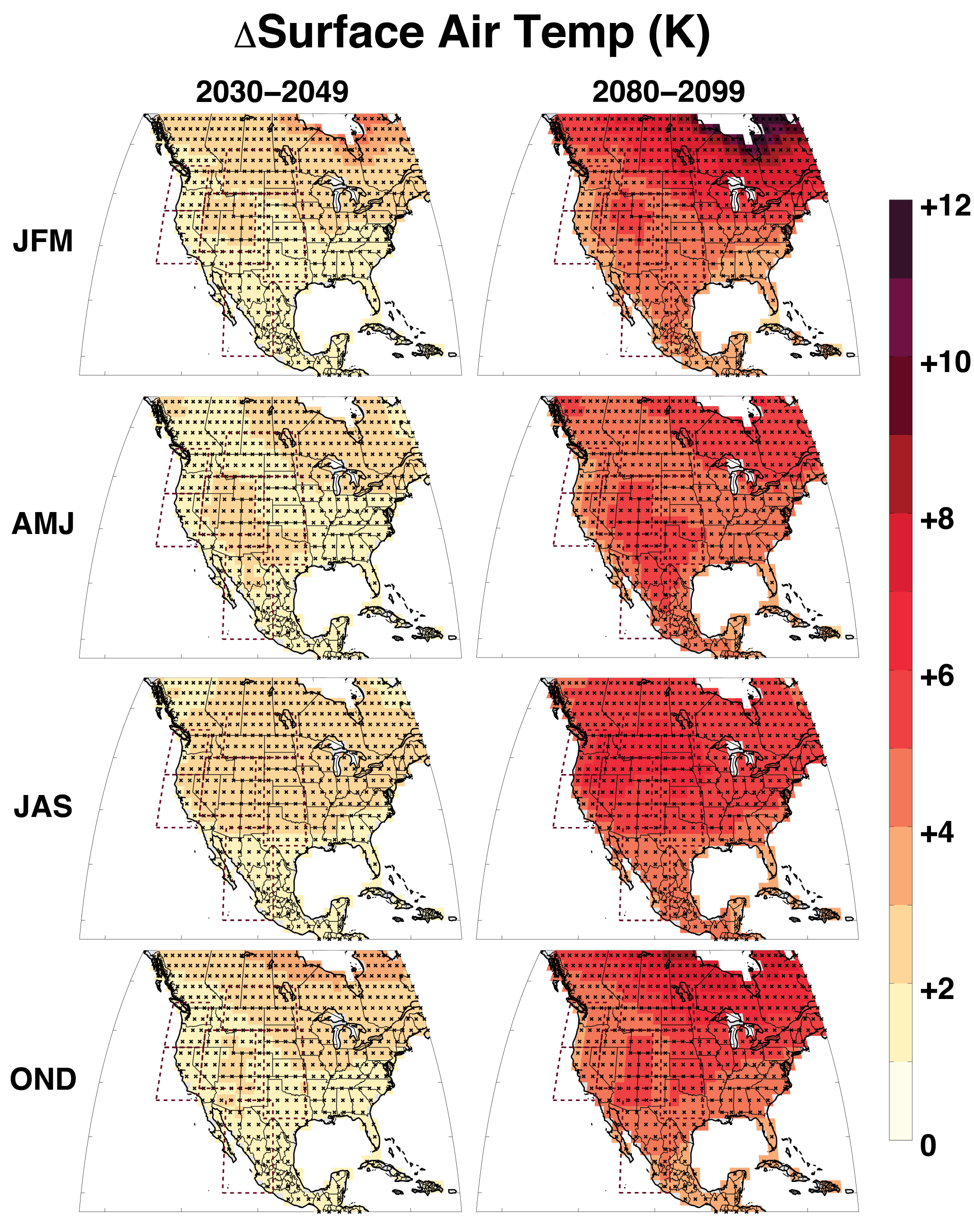

Fig. 3. Seasonally averaged multi-model mean surface air temperatures changes (K) in the RCP8.5 projections: 2030–2049 vs 1980-1999 (left column) and 2080–2099 vs 1980-1999 (right column). Areas marked with **x** indicate regions where changes in at least 18 of the 22 models (80%) agree with the sign of the change in the multi-model mean.

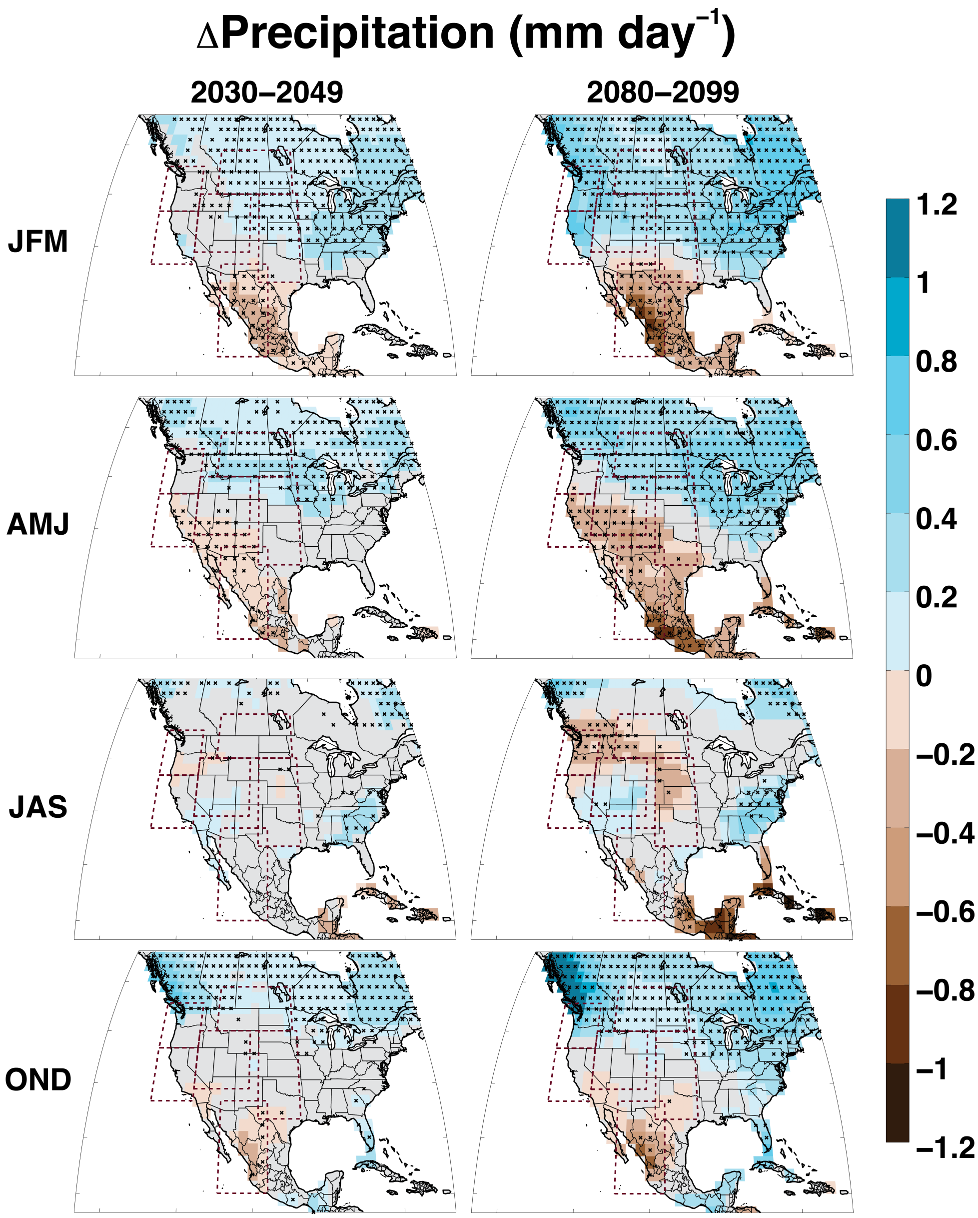

Fig. 4. Seasonally averaged multi-model mean precipitation (rain and snow) changes (mm day^{-1}) in the RCP8.5 projections: 2030–2049 vs 1980-1999 (left column) and 2080–2099 vs 1980-1999 (right column). Areas marked with **x** indicate regions where changes in at least 18 of the 22 models (80%) agree with the sign of the change in the multi-model mean. Small changes in the multi-model mean (< 5%) are masked out in gray.

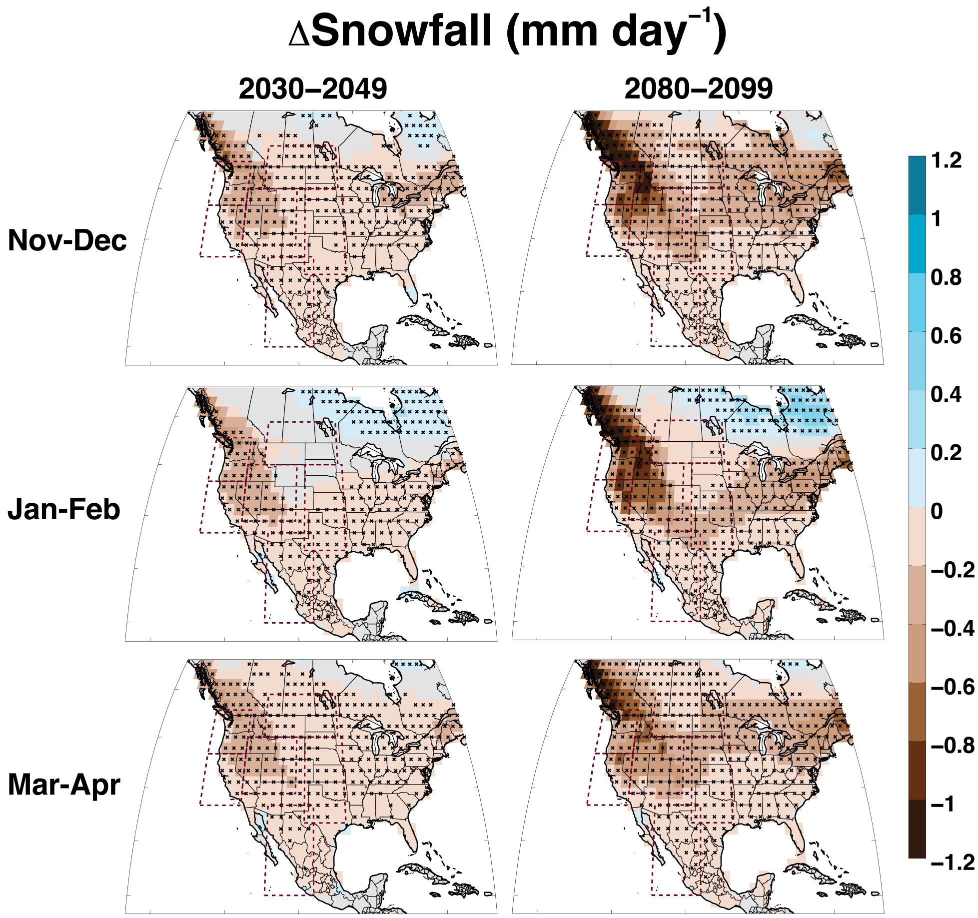

FIG. 5. Seasonally averaged multi-model mean snowfall changes (mm day^{-1}) in the RCP8.5 projections: 2030–2049 vs 1980-1999 (left column) and 2080–2099 vs 1980-1999 (right column). Areas marked with **x** indicate regions where changes in at least 18 of the 22 models (80%) agree with the sign of the change in the multi-model mean. Small changes in the multi-model mean (< 5%) are masked out in gray.

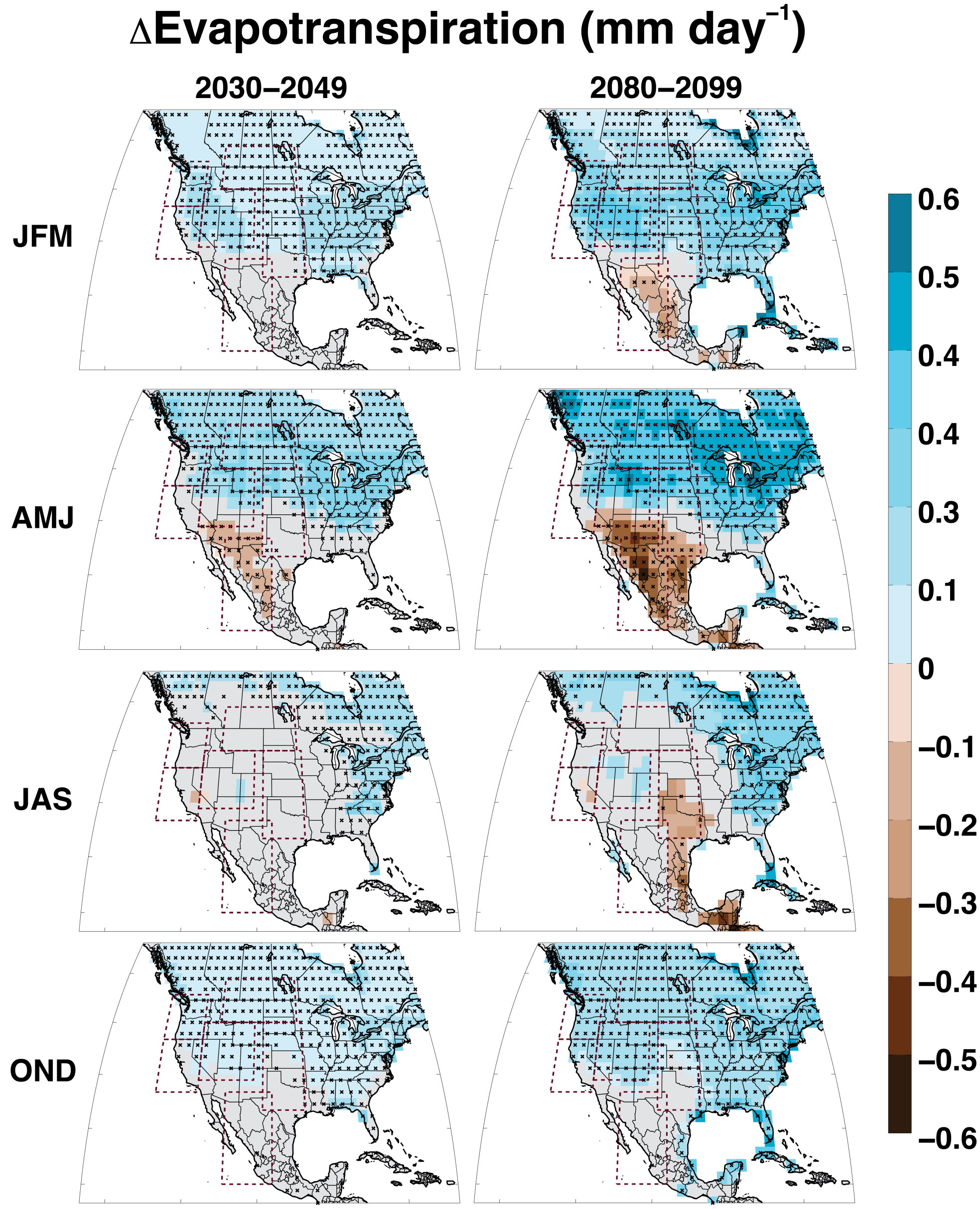

FIG. 6. Seasonally averaged multi-model mean evapotranspiration changes (mm day^{-1}) in the RCP8.5 projections: 2030–2049 vs 1980-1999 (left column) and 2080–2099 vs 1980-1999 (right column). Areas marked with **x** indicate regions where changes in at least 18 of the 22 models (80%) agree with the sign of the change in the multi-model mean. Small changes in the multi-model mean (< 5%) are masked out in gray.

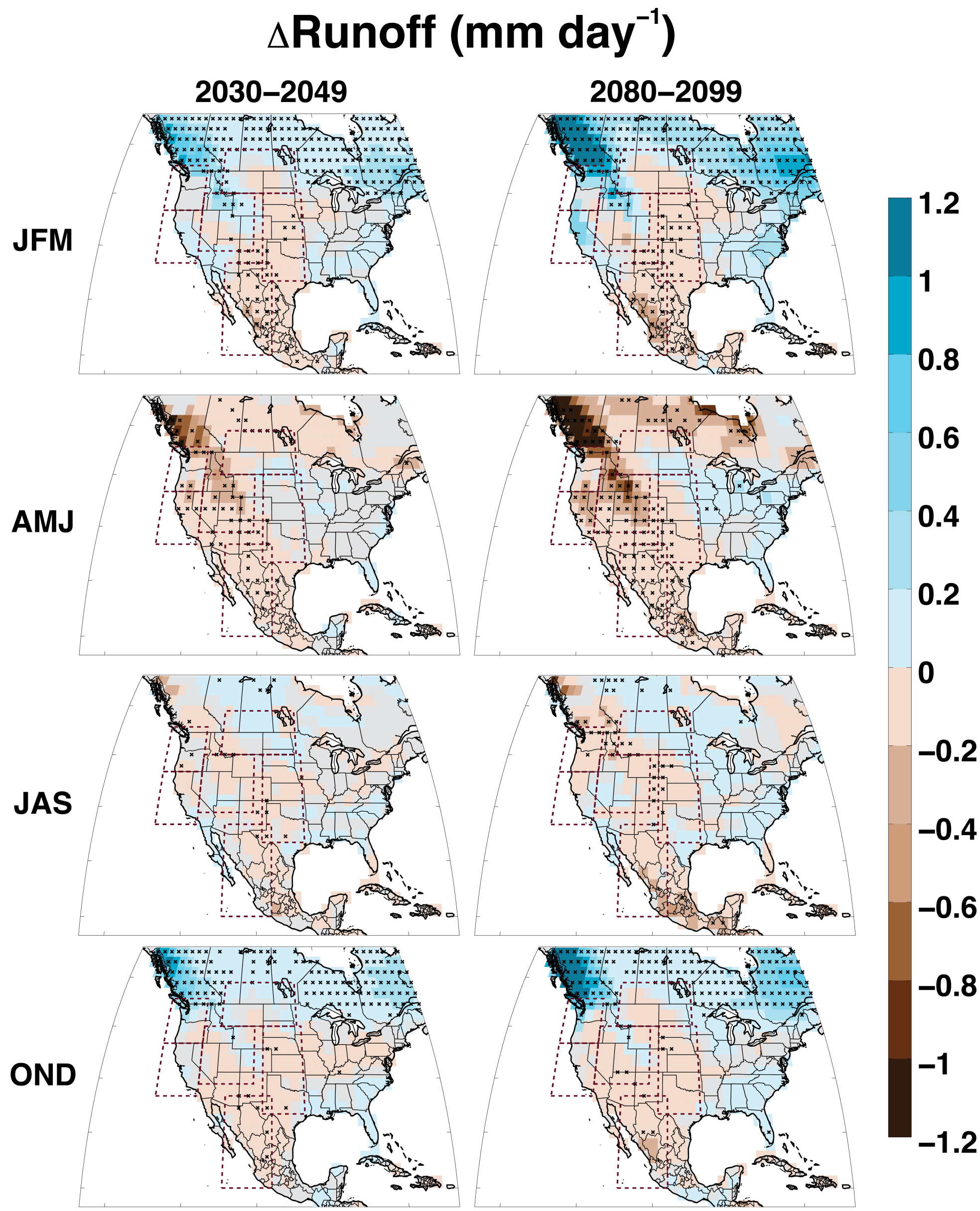

FIG. 7. Seasonally averaged multi-model mean runoff (surface and subsurface) changes (mm day^{-1}) in the RCP8.5 projections: 2030–2049 vs 1980-1999 (left column) and 2080–2099 vs 1980-1999 (right column). Areas marked with **x** indicate regions where changes in at least 18 of the 22 models (80%) agree with the sign of the change in the multi-model mean. Small changes in the multi-model mean (< 5%) are masked out in gray.

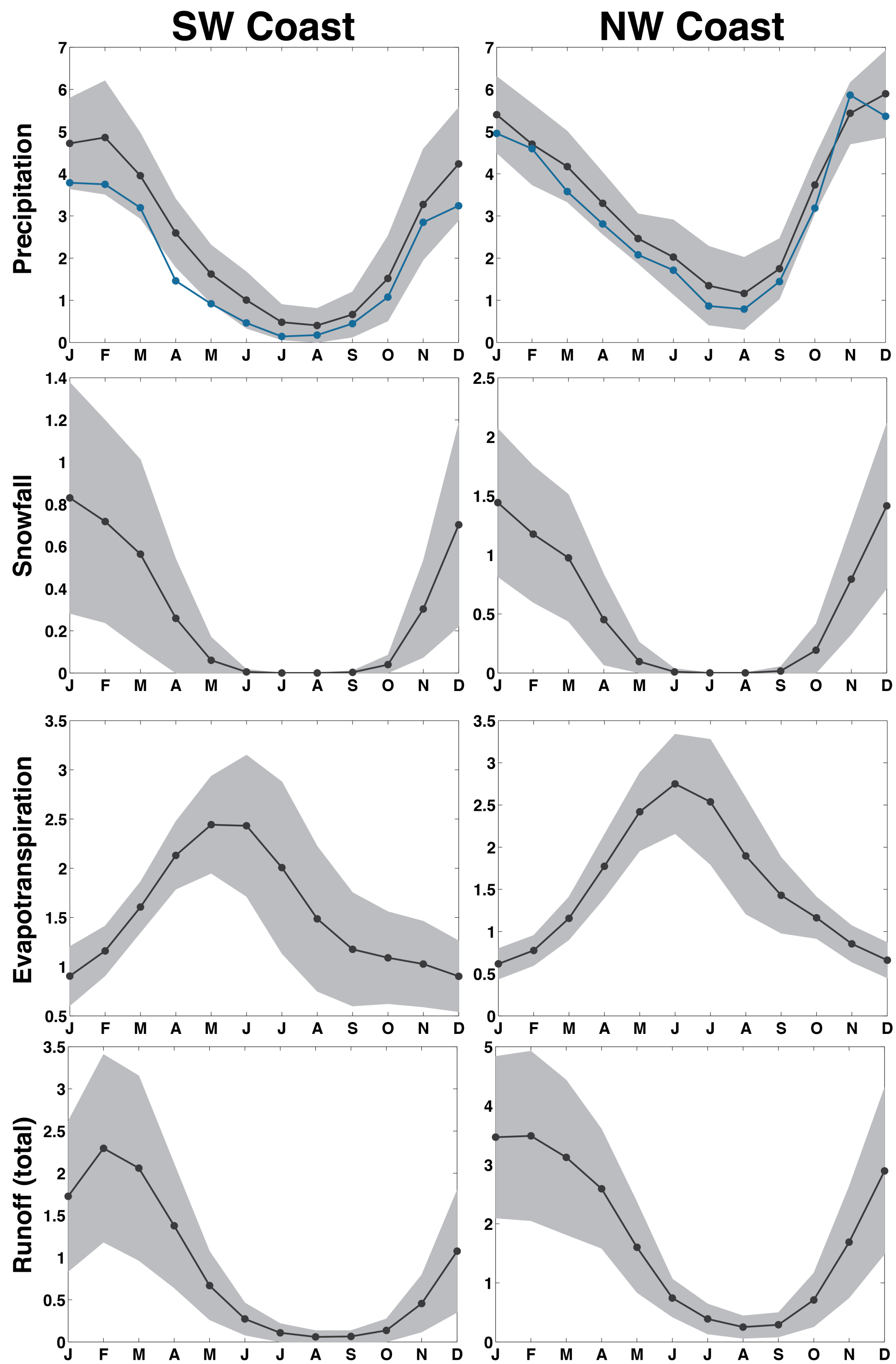

Fig. 8. Model climatologies (1980–1999, historical scenario) for the Southwest and Northwest coastal regions: precipitation, snowfall, evapotranspiration, and runoff. Units for all variables are mm day^{-1}. Solid black line is the multi-model mean, and the multi-model ensemble spread (+/-1 standard deviation) is indicated by the gray shading. Blue line in the precipitation panels is the observed climatology from the GPCC dataset, calculated for 1980–1999.

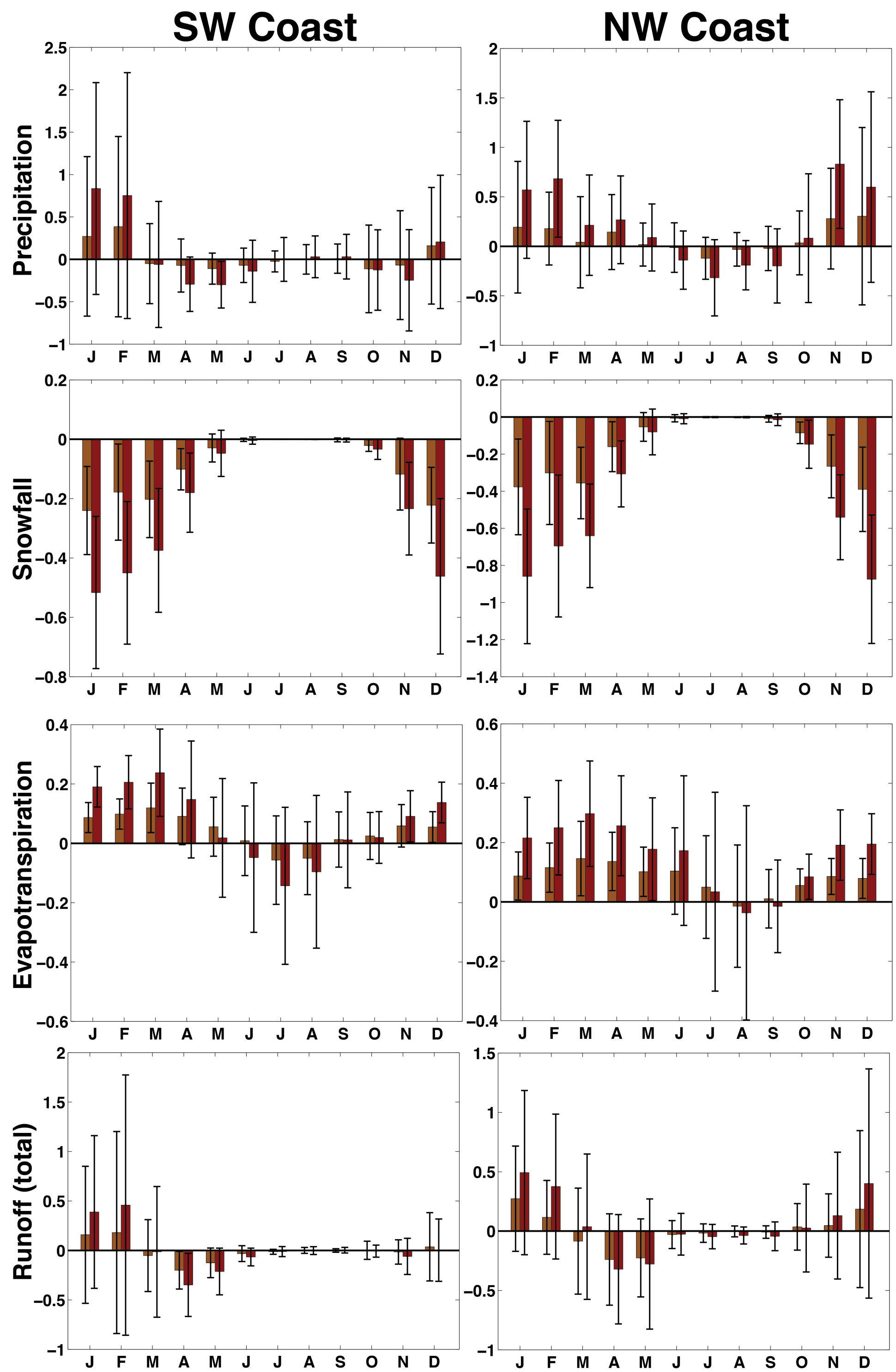

FIG. 9. Monthly changes in precipitation, snowfall, evapotranspiration, and runoff for the Southwest and Northwest coastal regions. Orange bars are the multi-model mean difference for 2030–2049 minus 1980–1999; red bars are for 2080–2099 minus 1980–1999. Whiskers indicate +/-1 standard deviation calculated across the 22 member multi-model ensemble.

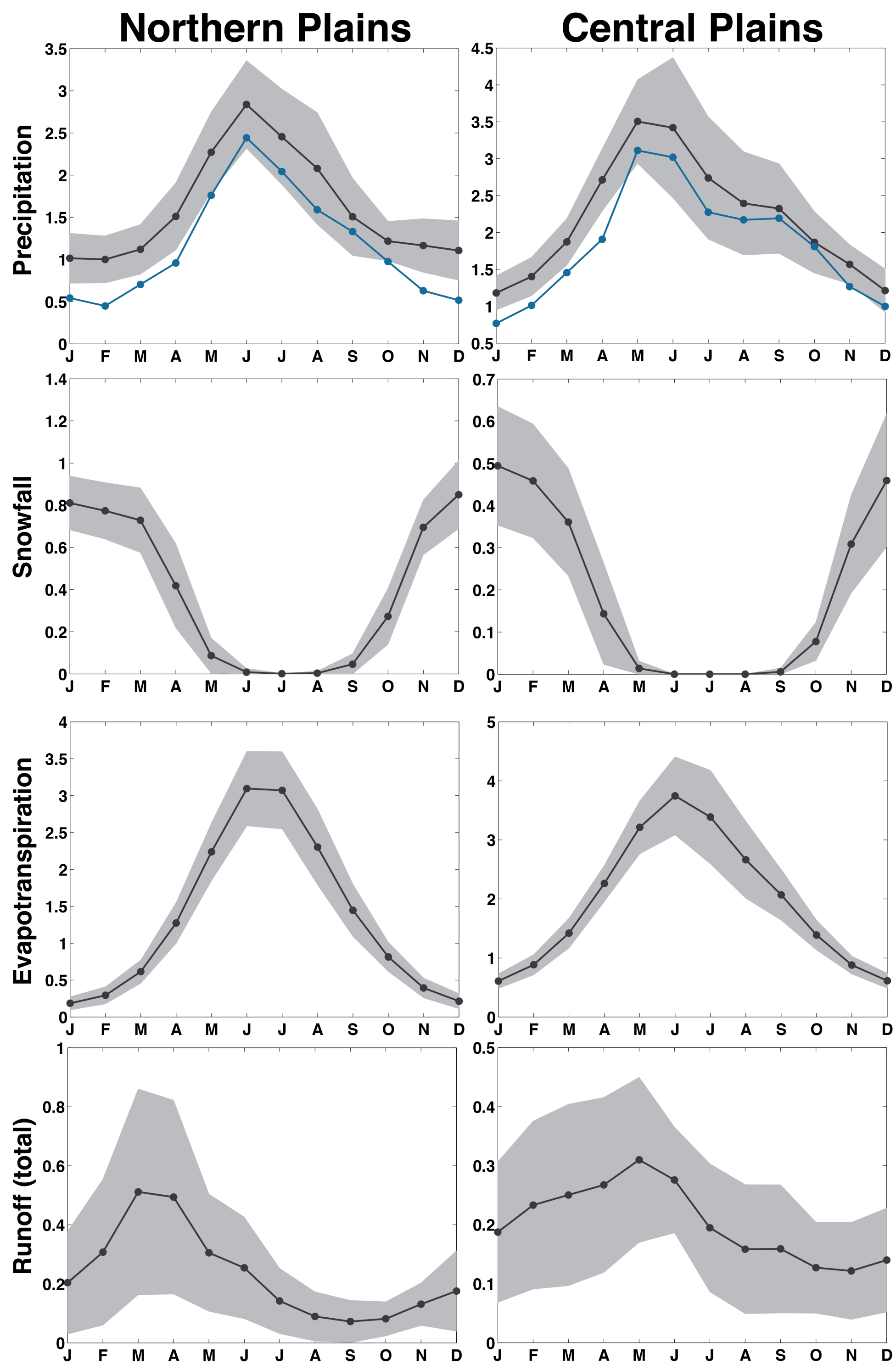

FIG. 10. Model climatologies (1980–1999, historical scenario) for the Northern and Central Plains regions: precipitation, snowfall, evapotranspiration, and runoff. Units for all variables are mm day^{-1}. Solid black line is the multi-model mean, and the multi-model ensemble spread (+/-1 standard deviation) is indicated by the gray shading. Blue line in the precipitation panels is the observed climatology from the GPCC dataset, calculated for 1980–1999.

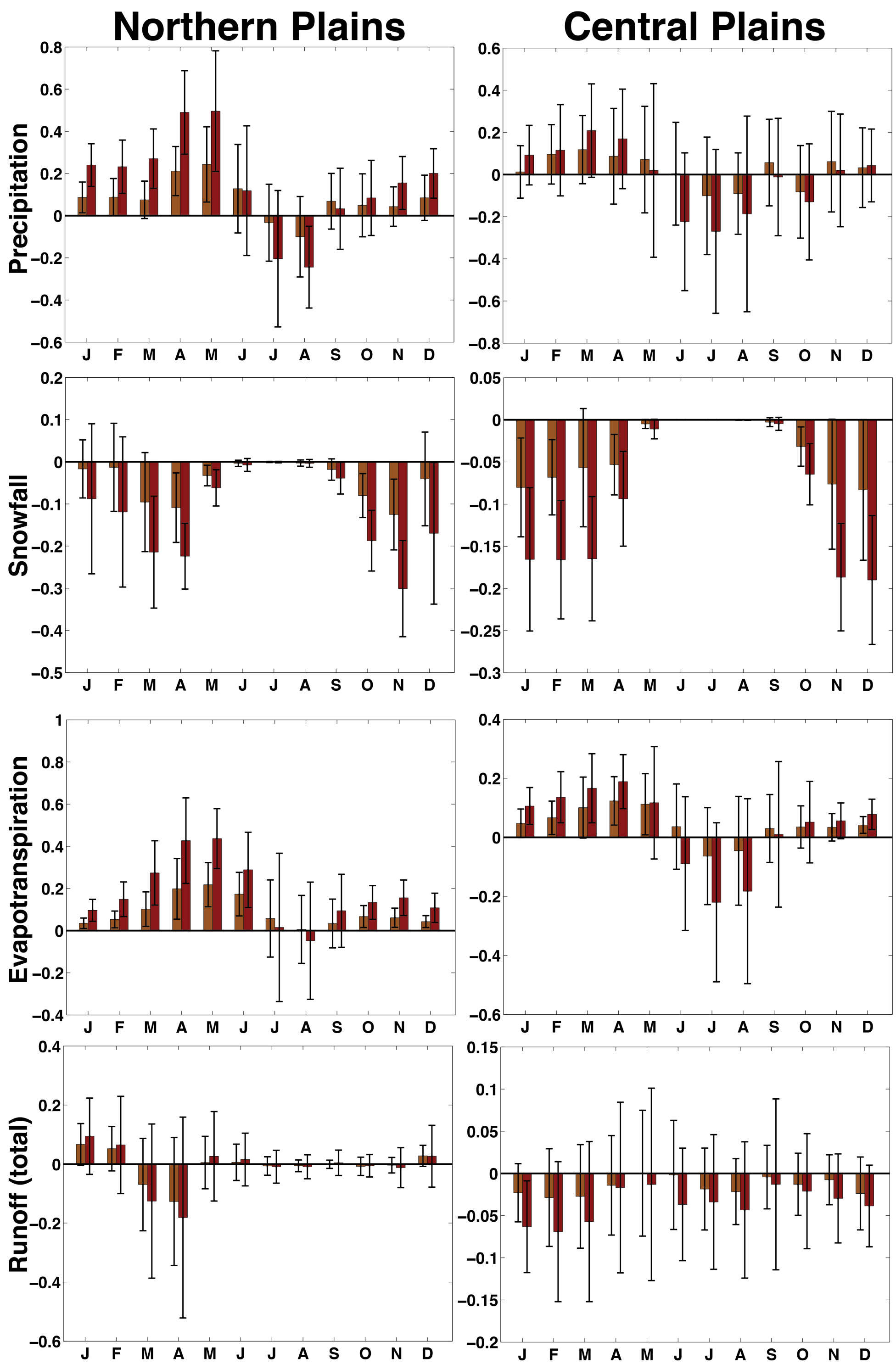

Fig. 11. Monthly changes in precipitation, snowfall, evapotranspiration, and runoff for the Northern and Central plains. Orange bars are the multi-model mean difference for 2030–2049 minus 1980–1999; red bars are for 2080–2099 minus 1980–1999. Whiskers indicate +/-1 standard deviation calculated across the 22 member multi-model ensemble.

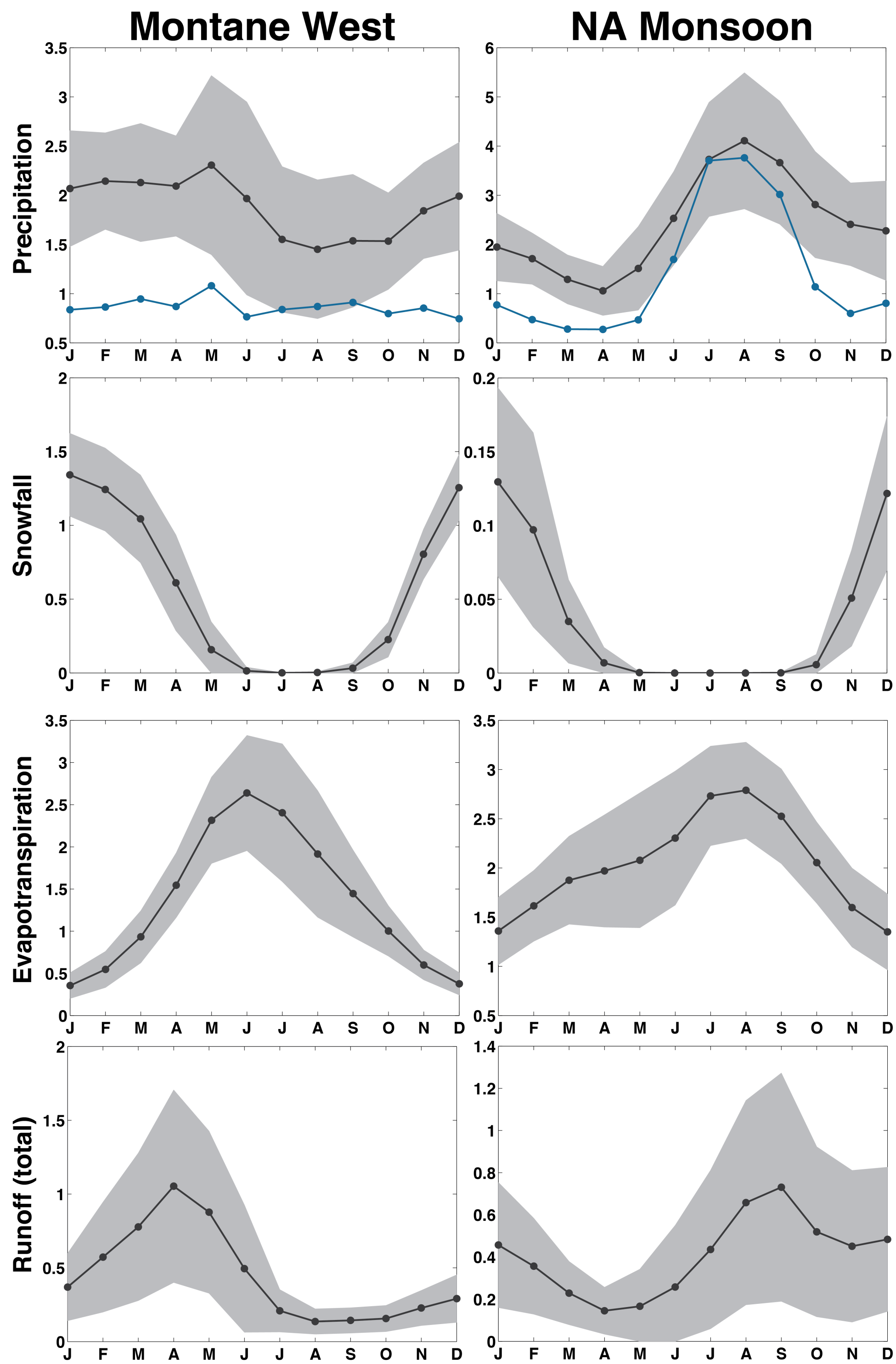

FIG. 12. Model climatologies (1980–1999, historical scenario) for the Montane West and North American Monsoon regions: precipitation, snowfall, evapotranspiration, and runoff. Units for all variables are mm day^{-1}. Solid black line is the multi-model mean, and the multi-model ensemble spread (+/-1 standard deviation) is indicated by the gray shading. Blue line in the precipitation panels is the observed climatology from the GPCC dataset, calculated for 1980–1999.

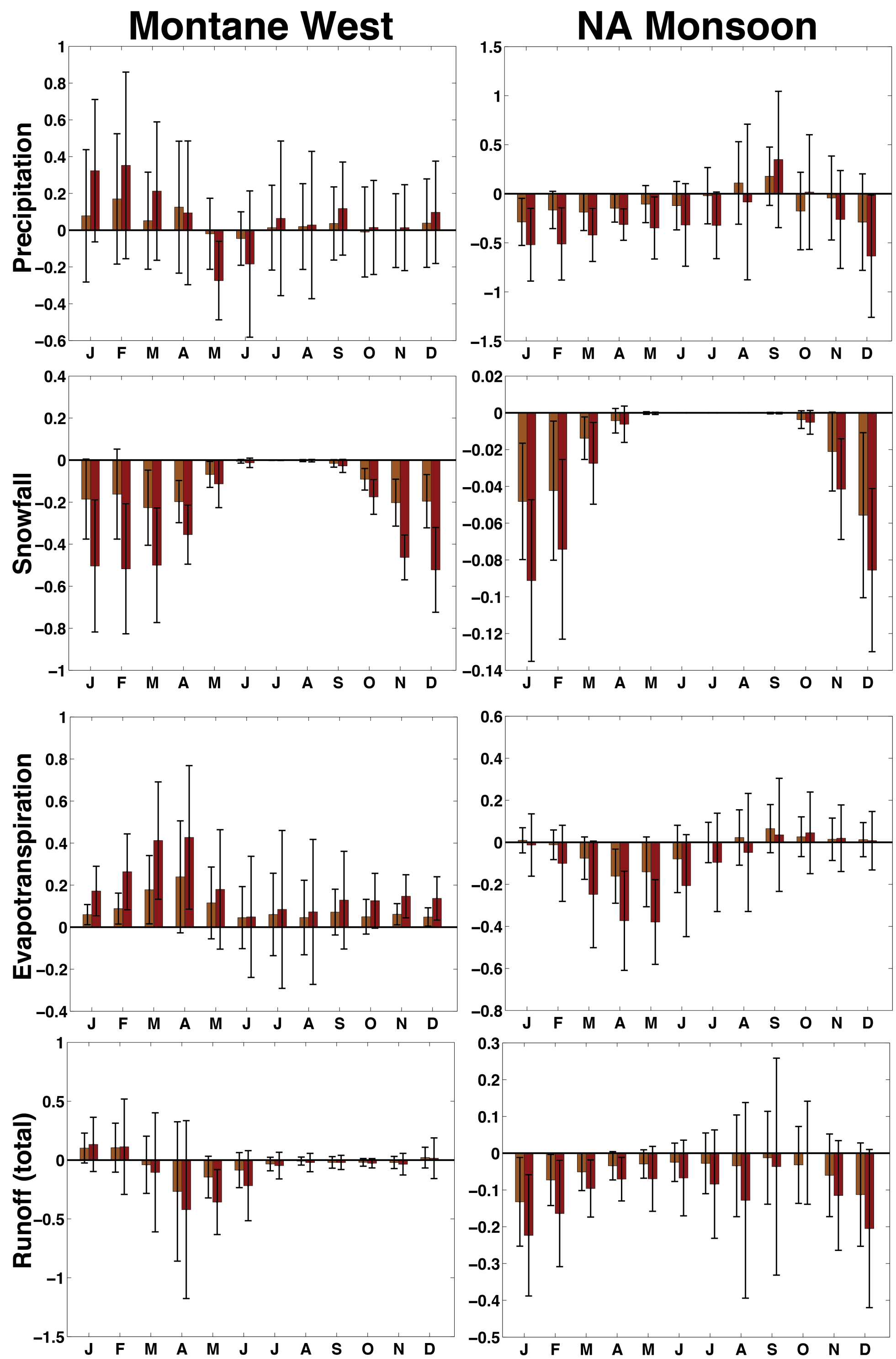

FIG. 13. Monthly changes in precipitation, snowfall, evapotranspiration, and runoff for the Montane West and North American Monsoon regions. Orange bars are the multi-model mean difference for 2030–2049 minus 1980–1999; red bars are for 2080–2099 minus 1980–1999. Whiskers indicate +/-1 standard deviation calculated across the 22 member multi-model ensemble.

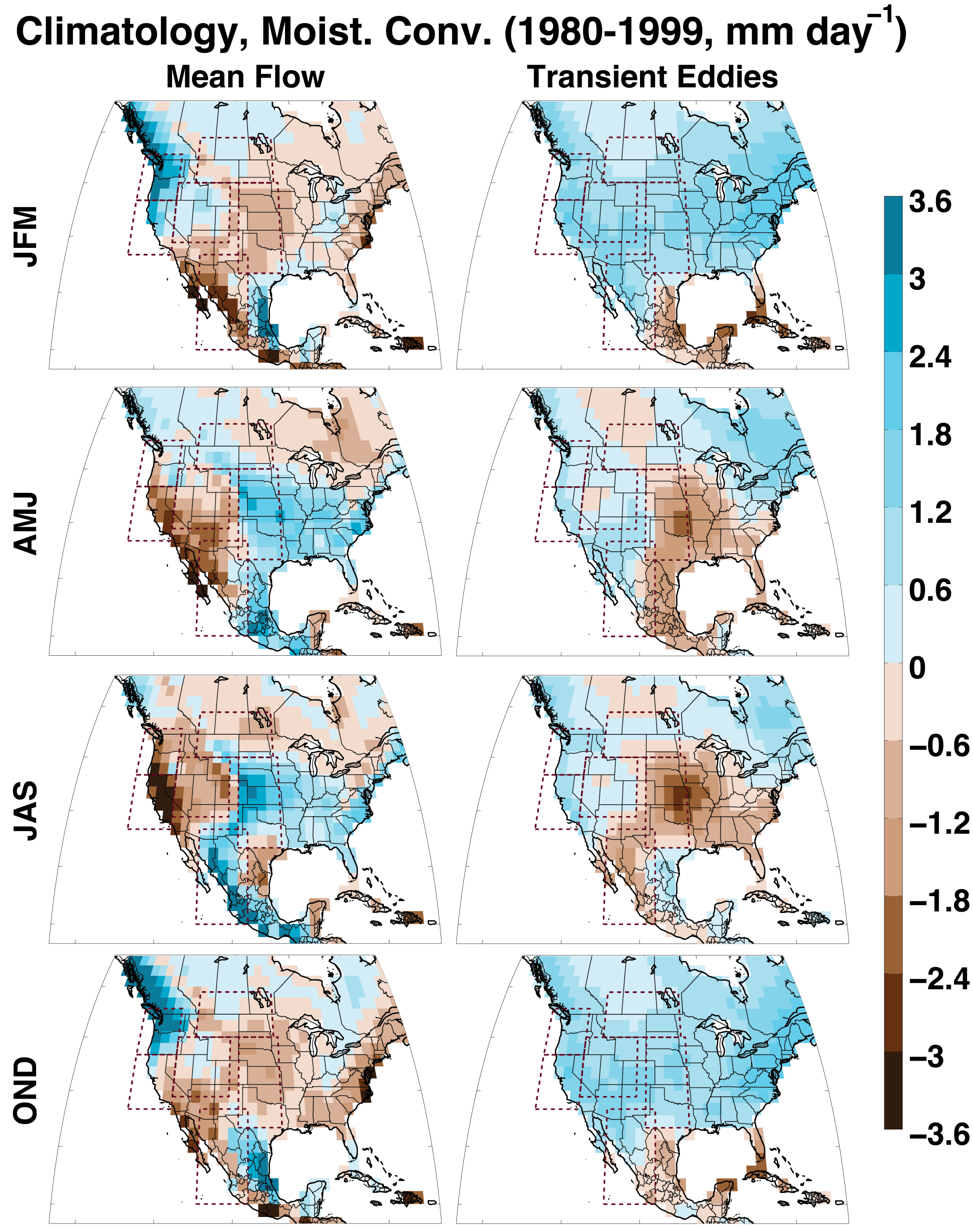

FIG. 14. Multi-model (17 models) mean climatology of seasonal moisture convergence (historical simulation, 1980–1999): mean flow (left column) and transient eddies (right column). Units are in mm day^{-1}.

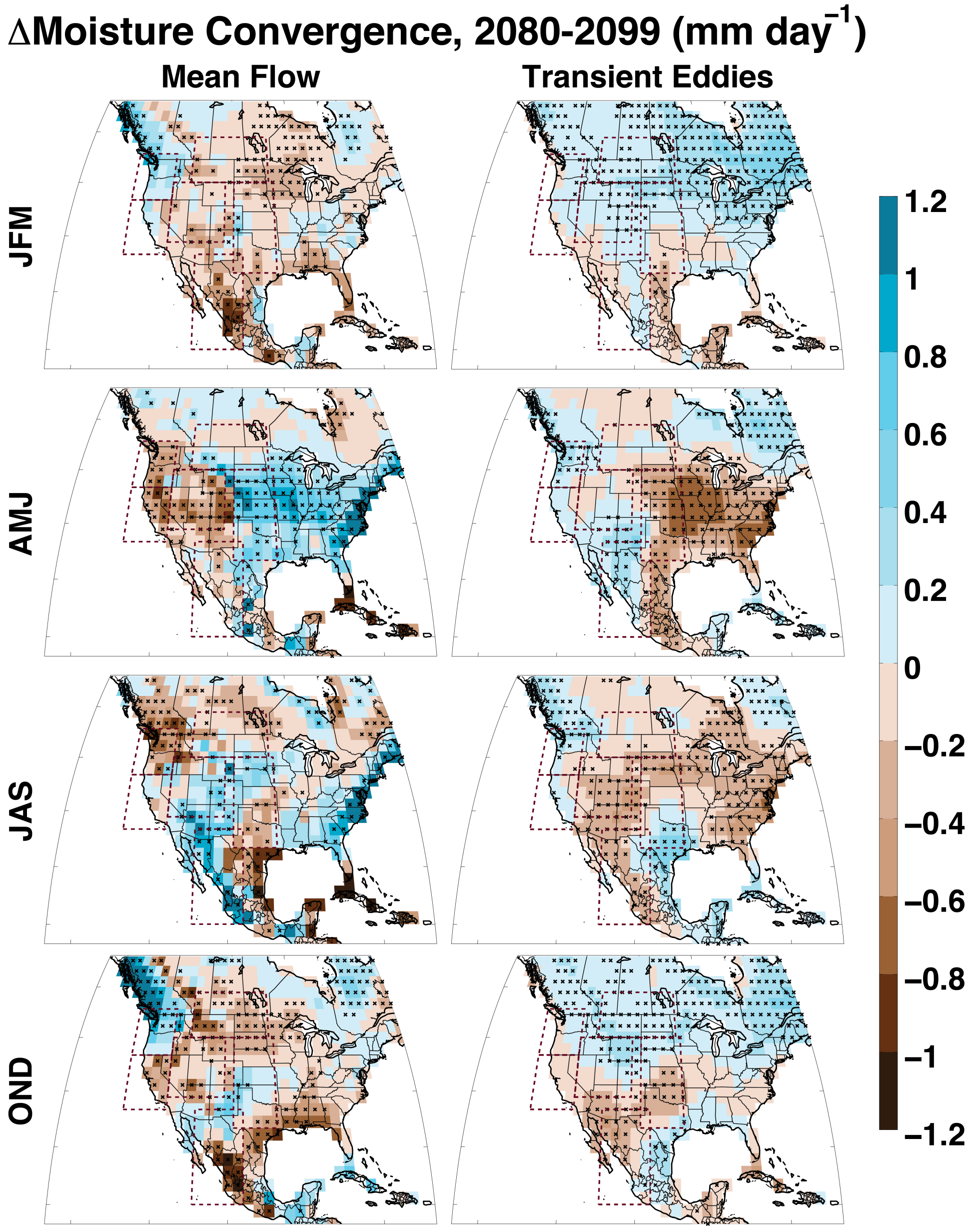

FIG. 15. Multi-model (17 models) mean changes in seasonal moisture convergence (2080–2099 minus 1980–1999) from changes in the mean flow (left column) and transient eddies (right column). Units are in mm day-1. Areas marked with **x** indicate regions where changes in at least 18 of the 22 models (80%) agree with the sign of the change in the multi-model mean. Small changes in the multi-model mean (< 5%) are masked out in gray.